

Experimental signatures of a new channel of the DD reaction at very-low energy

R. Dubey^{1,*}, K. Czerski¹, Gokul Das H¹, A. Kowalska², N. Targosz-Sleczka¹, M. Kaczmarski¹, and M. Valat¹

¹Institute of Physics, University of Szczecin, 70-451 Szczecin, Poland

²Institute of Mathematics, Physics and Chemistry, Maritime University of Szczecin, 70-500 Szczecin, Poland

*Corresponding author: rakesh.dubey@usz.edu.pl

Abstract

The discovery of a new, strong reaction channel of the deuteron-deuteron fusion at very low energies might have major consequences for the construction of a future clean and efficient energy source. Following the first theoretical and experimental indications for the existence of the deuteron-deuteron threshold resonance in the ${}^4\text{He}$ nucleus and its dominant decay by the internal e^+e^- pair creation, we present here an extensive experimental study confirming emission of high-energy electrons and positrons. A simultaneous use of Si charged particle detectors of different thicknesses and large volume NaI(Tl) and HPGe detectors has allowed for the first time to determine the branching ratio between emitted protons, neutrons and e^+e^- pairs for deuteron energies down to 5 keV. The high-energy positrons could be unambiguously detected by their bremsstrahlung spectra and annihilation radiation, supported by the Monte Carlo Geant4 simulations. The theoretical calculations, based on a destructive interference between the threshold resonance and the known broad resonance in ${}^4\text{He}$, agree very well with experimentally observed increase of branching ratios for lowering projectile energies. The partial width of the threshold resonance for the e^+e^- pair creation should be at least 10 times larger than that of the proton channel.

The fusion of helium nuclei via the deuteron-deuteron (DD) reactions is crucial not only for the understanding of primordial and stellar nucleosynthesis [1, 2] but also for the design and construction of next-generation clean energy sources [3]. While extensively studied for the last decades, intriguing indications for the existence of a 0^+ DD threshold resonance have recently been presented [3, 4]. One of the most important consequences of this resonance is that internal e^+e^- pair creation (IPC) should be the dominant reaction channel at deuteron energies lower than a few keV, which can entirely change our perception of fusion reactions for their commercial applications.

From a theoretical point of view [3], the existence of the threshold resonance is due to the weak coupling between $2+2$ and $3+1$ cluster states in the compound ${}^4\text{He}$ nucleus, which was already proposed in 1972 [5] and later supported by experimental results, as well as by multichannel R-Matrix parameterization [6]. This effect, however, still cannot be correctly reproduced in *ab initio* calculations [9, 8, 7, 10] which predict a significant contribution of the DD continuum to the first excited state 0^+ in ${}^4\text{He}$, being a cluster state of proton and triton, located about 3.6 MeV below the DD threshold [3]. In the case of strong coupling, the threshold DD resonance would merge with the first excited state as demonstrated in [11, 12], and the DD reaction would favor neutron and proton channels compared to the seven orders of magnitude weaker gamma emission.

Experimentally, measurement of the DD reactions at extremely low energies is very challenging not only because of dropping cross-sections but also due to atomic effects which can contribute to the yields of measured reaction rates. First of all, the enhanced electron screening effect, which is responsible for reducing the height of the Coulomb barrier between reacting nuclei, depends on the type of the crystal lattice structure as well as on the occurrence of the crystal lattice defects in hosting metallic target [4, 13, 14]. The electron screening effect leads to an exponential-like increase of the reaction probability when compared to the bare nuclei case. Additionally, the ion beam can be neutralized on the way to the target due to the large cross-sections of the ion charge exchange reaction with the vacuum atoms of the residual gas at very low energies.

However, all these effects can be controlled if a high-current accelerator with an ultra-high vacuum system can be applied [15]. The ability to supervise these processes was of particular importance when measuring the proton to electron ratio using the thin Si detector technique [16, 17], which allowed reducing systematic uncertainties. These measurements together with theoretical calculations and Geant4 MC simulations [18] could already deliver the first indications for a resonant production of electrons and positrons in the DD reactions [16, 17]. However, apart from relatively poor event statistics, any experimental arguments for the emission of high-energy positrons could not be provided.

Therefore, in this work, a much more reliable signature of a novel reaction channel in the DD fusion at ultra-low energies is presented. Following the initial observation, a two-year experimental campaign to gain deeper insights into the DD threshold resonance mechanism was conducted. To meticulously examine this new phenomenon, a long-lasting series of experiments was employed. In these experiments, various charged particle detector setups (Si detectors and Al absorption foils with varying thicknesses) at very low deuteron beam energies ranging between 5 and 20 keV were used. An important and crucial step was to measure for the first time photon emission being characteristic of the studied reaction mechanism, such as bremsstrahlung and annihilation radiations, using large-volume NaI(Tl) and HPGe detectors. The theoretical reaction model was further improved, leading to a much higher partial resonance width for the IPC decay.

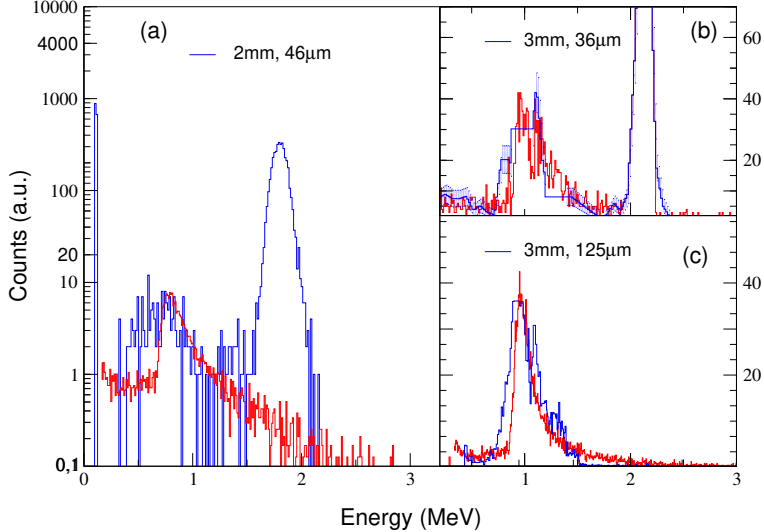


Figure 1: The experimental energy spectrum (in blue) measured at deuteron energy of 10 keV using (a) 2 mm thick Si detector with $36 \mu\text{m}$ absorption Al foil, (b) 3 mm thick Si detector with $46 \mu\text{m}$ absorption Al foil, and (c) 3 mm thick Si detector with $125 \mu\text{m}$ absorption Al foil. In the last case, the protons are fully absorbed in the Al foil. The Geant4 calculated spectrum is presented in red.

Charge particle spectra

Figure 1a-c displays the charge particle spectra obtained from 2 and 3 mm thick Si detectors following DD reactions at 10 keV deuteron beam energy. A prominent peak at 0.7 MeV and at around 1 MeV, measured with 2 mm and 3 mm Si detectors, respectively, correspond to the e^+e^- IPC according to the Geant 4 calculations (red curve). At higher energies, a 3 MeV proton line is also visible in Fig. 1a and 1b. Its exact energetic position depends on the thickness of the absorption Al foil placed in front of the detectors. The 36 and $46 \mu\text{m}$ thicknesses of the foils were enough to fully absorb 1.2 MeV tritons and 0.9 MeV ^3He particles, so they are not visible in the spectra. In the case of the thickest, $125 \mu\text{m}$ Al foil (Fig. 1c), the proton line also disappears. In this configuration, only a distinct e^+/e^- peak persists around 980 keV due to their much lower stopping power values.

As already discussed in [16, 17], the position of the e^+/e^- peak corresponds to the partial energy deposition of high-energy electrons/positrons within Si detectors, which are not thick enough to absorb their full energy. As the stopping power functions of electrons and positrons are very similar and change only slightly in the energy range of 1-20 MeV, the peak position corresponds to the thickness of the detector. Detailed calculations of the electron/positron spectra were performed, taking into account both the continuous e^+e^- energy distributions arising from the IPC $0^+ \rightarrow 0^+$ transition to the ground ^4He state, as well as the comprehensive Geant4 Monte Carlo (MC) simulations of the experimental setup [17]. The slight discrepancy observed in the peak position of the simulated versus measured electron spectrum can be attributed to non-uniformities in the depletion region of the thicker Si surface barrier detectors. To account for this effect, a correction of approximately

10 percent for 2 mm and 3 mm thick detectors was incorporated into the simulations.

It is important to emphasize that the e^+e^- peak couldn't be observed in previous measurements performed by many authors since they used thinner Si detectors (of the order of 100 μm) to improve the effect/noise ratio (see Fig. 6) [4]. In that case, the e^+e^- absorption peak would lie at energy of about 30 keV, being below the noise threshold of Si detectors, disabling its observation.

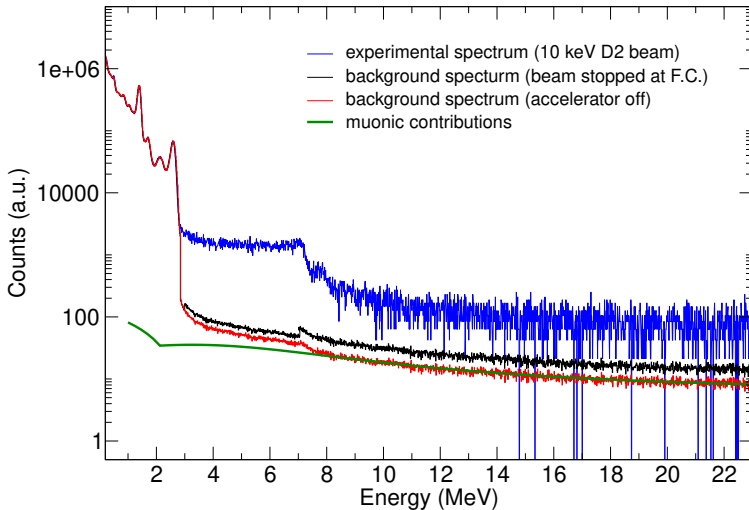


Figure 2: Experimental gamma spectrum (blue curve) measured with a 10 keV deuteron beam on the ZrD_2 target, compared to background measurements obtained when the accelerator was fully turned off (red curve) and with the beam stopped at the Faraday cup (black curve). The green solid line shows the estimated cosmic muonic contributions. [19, 20]

NaI(Tl) photon spectra

In parallel with the measurements of the charged particles, the detection of photons originating from the 23.84 MeV IPC process was performed. A large volume cylindrical sodium iodide (NaI(Tl)) detector (20 cm in diameter and 25 cm long) coupled to 4 photomultipliers was integrated into the experimental setup. The experimental gamma spectrum recorded during irradiation of a deuterated Zr target (ZrD_2) with a 10 keV deuteron beam is shown in Fig. 2. For comparison, two background spectra are also plotted. One spectrum was measured with the deuteron beam placed on the Faraday cup in front of the target chamber and the other one when the accelerator was turned off. For the detection of bremsstrahlung induced by high-energy electrons/positrons, the high-energy region above 9 MeV is especially important. Due to the electromagnetic noise, the count rate obtained in this energy region with the beam on the Faraday cup is about 73 percent higher than that measured without the accelerator, being mainly induced by cosmic muons. The gamma spectra below 3 MeV are dominated by natural radioactivity of ^{40}K (1462 keV line) and ^{208}Tl (2615 keV line). In the intermediate energy region 3-9 MeV, a strong contribution induced by the 2.3 MeV neutrons from the $^2\text{H}(\text{d},\text{n})^3\text{He}$ reaction is visible. All the components of the energy spectra compared to the Geant4 MC simulation calculations are depicted in detail in Fig. 3 (a, b). The neutron induced spectrum, showing several well resolved discrete transitions, could be easily iden-

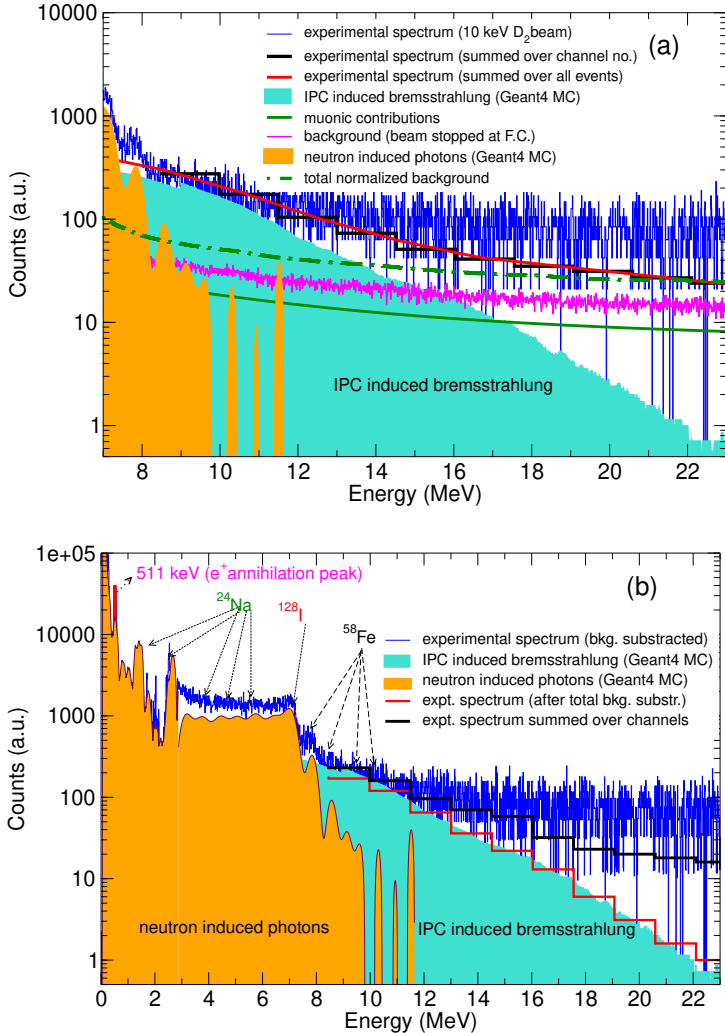


Figure 3: (a) Decomposition of the high photon energy spectrum measured by a large cylindrical NaI(Tl) detector at a deuteron energy of 10 keV (blue curve). The black step curve represents the experimental spectrum summed over more pulse-height channels to reduce statistical fluctuation. The background contributions resulting from cosmic muons (violet curve) and that increased due to the electromagnetic noise obtained with the beam on the Faraday cup (green curve) and in the target chamber (magenta curve) are also depicted. The strength of the Geant4 Monte Carlo bremsstrahlung spectrum induced by the IPC electrons/positrons (green color area) has been fitted to the experimental spectrum (red curve). The neutron induced contribution (yellow color area), calculated using the Geant4 MC simulation is displayed as well. (b) Decomposition of the full photon energy spectrum measured by a large cylindrical NaI(Tl) detector at a deuteron energy of 10 keV after subtraction of the natural muonic background (blue curve). The black step curve represents the experimental spectrum summed over more pulse-height channels to reduce statistical fluctuation and the red step curve is the same spectrum obtained after subtraction of the full background (magenta line in Fig 3a).

tified. Especially challenging was, however, determination of the bremsstrahlung contribution at energies above 9 MeV resulting from stopping of high-energy IPC electrons and positrons. To reduce statistical uncertainties, the high-energy photon spectrum was first summed over more pulse-height channels (black step curve in Fig. 3) and then, after taking into account the background contribution, the amplitude of the bremsstrahlung spectrum could be fitted. The experimentally observed decrease of the counting rate at high energies (above 9 MeV) agrees very well with

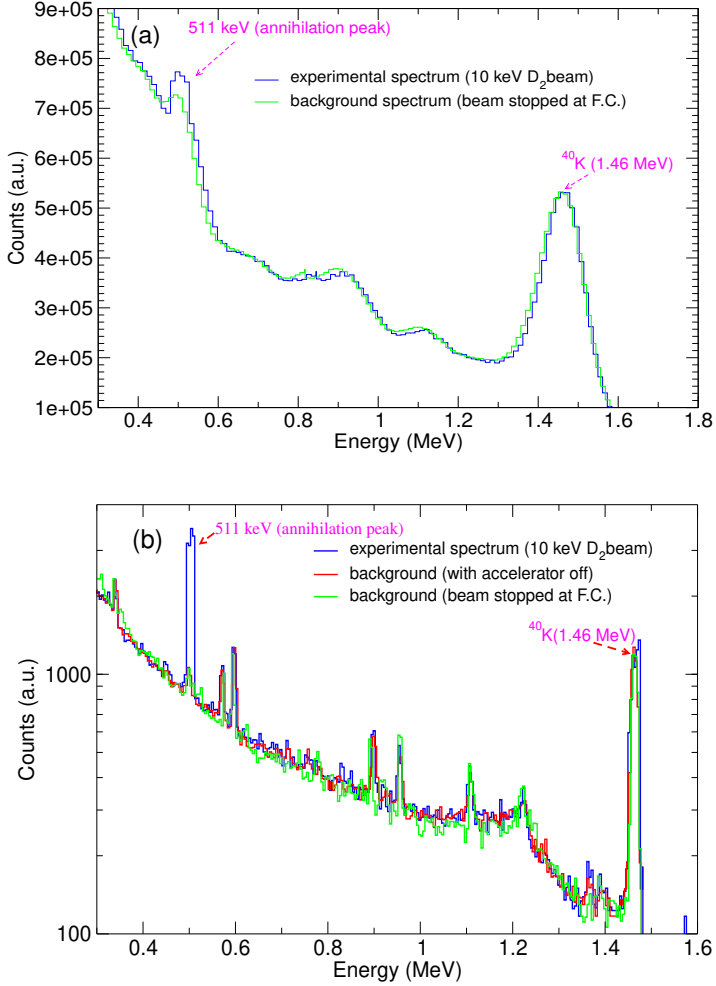


Figure 4: (a) Low energy gamma spectra measured with the NaI(Tl) detector. The red curve corresponds to the background measurement performed with the deuteron beam on the Faraday cup. The blue curve represents the effect obtained during irradiation (10 keV deuteron beam) of the deuterated Zr target. (b) Low energy gamma spectra measured with the HPGe detector. The spectrum obtained for the deuterated Zr target irradiated with a 10 keV deuteron beam is compared to the background measurements taken either with the ion beam on the Faraday cup or with the accelerator turned off.

the result of the Geant4 calculations. The strength of the bremsstrahlung contribution corrected by the NaI(Tl) detector efficiency has been used for calculations of the branching ratio between e^+e^- pair creation and the number of emitted protons measured independently by the Si detector (see Table 1).

A similar procedure has been employed to estimate the neutron flux from the DD reaction. As shown in Fig. 4, photon peaks (at 1.37, 2.75, 4.5, 5.7, and 6.4 MeV) induced by the $^{23}\text{Na}(n,\gamma)^{24}\text{Na}$ reaction on the NaI(Tl) detector are easy to identify, as well as the line at 6.9 MeV, resulting from $^{127}\text{I}(n,\gamma)^{128}\text{I}$ [22]. The peaks attributed to the μ -metal (75 percent nickel, 20 percent iron) chamber with high (n,γ) cross-sections of ^{56}Fe (92 percent natural abundance) at 7.645 MeV and other peaks between 8-10 MeV could be recognized. Overall, according to Geant4 MC simulations, the major contributions of neutron-induced photons in the measured spectra are dominant below 9 MeV, with almost negligible effects of reaction-induced

neutrons beyond this energy region.

Positron annihilation spectra

In the case of the internal e^+e^- pair emission, an excess of counts in the 511 keV annihilation line should be observed by both NaI(Tl) and HPGe detectors under deuteron irradiation of the ZrD₂ target. The corresponding spectra measured with the 10 keV deuteron beam and the background measurement without running the accelerator are presented in Fig. 4(a, b). The excess of 511 keV counts is clearly observed, although a large background contribution is also visible. As the strength of the background annihilation line does not change, even the deuteron beam is placed on the Faraday cup in front of the target chamber. Therefore, its origin seems to be natural and not due to the external pair creation of gamma radiation induced by neutrons from the DD reactions. This is also in agreement with Geant4 MC simulations which predict two orders of magnitude lower annihilation line intensity than the excess effect measured. Taking into account the absolute efficiency of detectors (see the Method Section), the branching ratio of the IPC process compared to the proton or neutron channel could be estimated. In the deuteron energy region studied, both nucleon reaction channels are assumed to be equal. On the other hand, if two different reaction channels can be investigated using the same detector, the systematic uncertainties of their branching ratio related to the detector positions can be neglected. The experimentally determined branching ratios based on the strength of the annihilation line are comparable to the values obtained using other methods (see Table 1) and strongly support the IPC process. Their values are significantly larger for the deuteron energy of 10 keV than for 20 keV in agreement with the results obtained with Si detectors.

Table 1: Experimentally determined branching ratios (BR): IPC/proton using 3 mm Si detector, IPC/neutron, and annihilation peak (AP)/neutron using both large volume NaI and HPGe detectors at deuteron energies of 10 and 20 keV, compared to theoretical calculations.

Deuteron Energy (keV)	BR (expt.)				BR (theory)
	IPC/proton (3 mm Si Det.)	IPC/neutron (Brms.)	AP/neutron (NaI Det.)	AP/proton (HPGe)	
10	0.42 ± 0.05	0.83 ± 0.06	1.70 ± 0.08	1.10 ± 0.05	0.245
20	0.060 ± 0.012	0.09 ± 0.05	0.16 ± 0.03	0.12 ± 0.06	0.042
10/20 ratio	7.0 ± 1.6	9 ± 5	10 ± 5	9 ± 3	5.8

Theoretical calculations

The experimental electron-proton branching ratio determined for the deuteron energies at 5-20 keV using 1-3 mm thick Si detectors with different Al absorber foils is shown in Fig. 5. A methodology adopted for the branching ratio calculation is well discussed in our recent studies [16, 17]. An increase of its value for the lowering deuteron energy related to the DD threshold resonance is clearly visible.

The excitation of this resonance has been previously observed in the $^2\text{H}(\text{d},\text{p})^3\text{H}$ reaction on both metallic and gaseous targets [4, 3]. This allowed the proton cross-section to be well described as the sum of two components: one corresponding to the well-known overlapping broad resonances in ^4He and the second describing the

narrow-threshold resonance [16]:

$$\sigma_p = \frac{\pi}{k} P(E+U_e) \left[\frac{k}{\pi} \frac{1}{\sqrt{EE_G}} S_p(E) + \frac{2\hbar^2}{\mu a} \frac{\Gamma_p}{E^2} + \left(\frac{k}{\pi} \frac{S_p(E)}{3} \frac{1}{\sqrt{EE_G}} \cdot \frac{2\hbar^2}{\mu a} \frac{\Gamma_p}{E^2} \right)^{1/2} \cos(\varphi_p^{0+}) \right], \quad (1)$$

where k , E , E_G and a denote for the wave number, the deuteron energy in CMS, and the Gamow energy and channel radius respectively. Your sentence is mostly clear but could be slightly refined for better readability. In the present calculation, $a = 7$ fm and the Gamow energy, E_G was considered to be 986 keV.

The penetration factor describes the s-wave penetration probability through the Coulomb barrier reduced by the electron screening energy U_e and it can be expressed as:

$$P(E + U_e) = \sqrt{\frac{E_G}{E + U_e}} \exp \left(-\sqrt{\frac{E_G}{E + U_e}} \right) \quad (2)$$

The broad resonance component (the first term in brackets in Eq. 1) can be determined from the known astrophysical S-factor for the proton channel equal to about 57 keV.b at very low deuteron energies. The second term results from the Breit-Wigner formula for the threshold resonance, assuming that the deuteron partial width takes on the maximum value of the single-particle resonance [4]. This relation could be simplified as the resonance energy is close to zero and therefore much smaller than the deuteron energy. The interference (third) term corresponds to the fact that only one third of the broad resonance transition goes through the 0^+ compound nucleus state and can interfere with the threshold resonance [3]. The proton partial width of the threshold was experimentally estimated to $\Gamma_p = 40$ meV and the nuclear phase shift of the broad resonance component to $\varphi_p^{0+} = 115^\circ$.

The cross-section for the e^+e^- pair creation can be calculated similarly to the proton channel (see Eq. 1), leading to an expression where Γ_{IPC} , Γ_p , and S_{IPC} should be fitted to the experimentally determined electron-proton branching ratio. Since the penetration factors for both channels are the same, the branching ratio will be independent of the electron screening energy. Differently from the previous calculations [16, 21] we consider here that a small IPC component of known broad resonances S_{IPC} exists and can interfere with the IPC contribution of the threshold resonance.

The theoretical calculations for different values of parameters are presented in Fig. 5. The best fit could be achieved for the ratio $\Gamma_{\text{IPC}}/\Gamma_p = 14$, $S_{\text{IPC}} = 0.25$ keV.b, and $\varphi_p^{0+} = 170^\circ$, assuming $\Gamma_p = 20$ meV. The theoretical curve was especially sensitive to the choice of the nuclear IPC phase shift. Due to its large value, the destructive interference for the IPC channel reaches its almost maximum value. On the other hand, small changes in the proton partial resonance width do not influence the fit quality significantly within the range of the experimental data. Only differences can be observed at deuteron energies below 2 keV. A small IPC contribution arising from the broad resonances was necessary to obtain a better fit to the new experimental data, which simultaneously leads to an approximately six times

higher $\Gamma_{\text{IPC}}/\Gamma_p$ ratio than determined before.

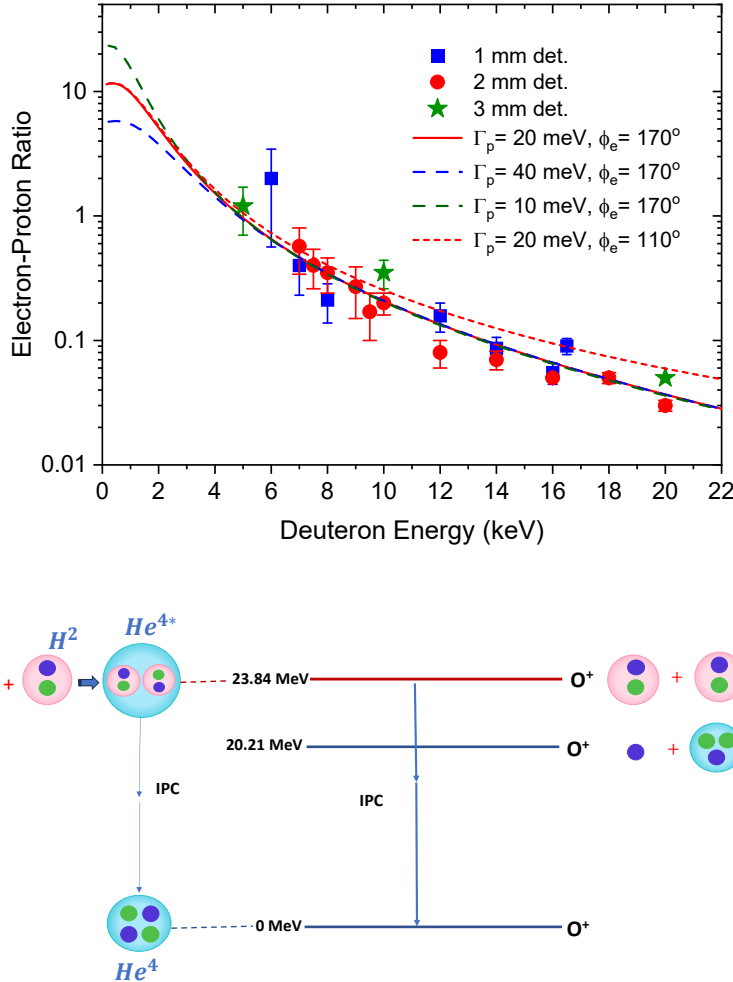


Figure 5: (a) Experimentally determined IPC/proton branching ratio compared to the theoretical calculations assuming different proton partial width of the DD threshold resonance and the phase shift of the broad resonance contribution. (b) Schematic visualization of the nuclear level scheme of ${}^4\text{He}$, showing deexcitation of the DD threshold resonance via IPC to the 0^+ ground state.

In summary, we present new measurements of the $\Gamma_{\text{IPC}}/\Gamma_p$ branching ratio of DD reactions down to the lowest deuteron energy of 5 keV, strongly increasing the number of experimental points and reducing their statistical uncertainties. We have used simultaneously charged particle Si-detectors of different thicknesses and large volume NaI(Tl) and HPGe detectors to measure emitted photons. Based on Geant4 Monte Carlo simulations, we could demonstrate that the broad maximum in the charged particle spectrum can be related to the e^+e^- partial absorption energy in Si detectors. The most impressive spectrum has been obtained with a $125\ \mu\text{m}$ thick aluminum placed in the front of a detector, which was enough to stop 3 MeV protons and measure only light charged particles (see Fig. 1). The large volume NaI(Tl)

detector could measure photons produced by capture of neutrons emitted in the DD fusion as well as a small contribution of high-energy bremsstrahlung photons, confirming emission of electrons or positrons with energy up to 23 MeV. An unambiguous proof for emission of positrons is observation of an excess in the 511 keV annihilation line. The photonic data are in a very good agreement with spectra obtained with Si detectors and confirm a strong increase of the IPC/proton branching ratio for lowering deuteron energies (see Fig. 5). The improved theoretical calculations can explain the experimental results with excitation of the DD single-particle threshold resonance observed previously in the $^2\text{H}(\text{d},\text{p})^3\text{H}$ reaction [4, 3]. The calculations of the branching ratio have considered for the first time an interference effect in both studied reaction channels, which has led to a much higher ratio of partial resonance widths, $\Gamma_{\text{IPC}}/\Gamma_p = 14$ than that determined before. The obtained results demonstrate that the strongest reaction channel of the DD fusion for deuteron energies below 5 keV is the internal e^+e^- pair creation, which can help in construction of future fusion energy sources if proper materials with a large electron screening energy could be utilized. The internal pair creation should be also involved in nuclear reaction rate calculations for astrophysical plasmas [23, 24].

Acknowledgments

This project has received funding from the European Union’s Horizon 2020 research and innovation program under grant agreement No 951974.

References

- [1] Fowler, W.A.: *Rev. Mod. Phys.* 56, 149 (1984).
- [2] C. Rolfs, Rodney, W.S.: *Cauldrons in the cosmos*. Chicago: University of Chicago Press (1988).
- [3] K. Czerski, *Phys. Rev. C (Letters)* 106, L011601 (2022).
- [4] K. Czerski, et al., *Europhys. Lett.* 113, 22001 (2016).
- [5] V.A. Sergeyev, *Phys. Lett. B* 38, 286 (1972).
- [6] D.R. Tilley, H. R. Weller, and G. M. Hale, *Nucl. Phys. A* 541, 1 (1992).
- [7] A. Csótó and G. M. Hale, *Phys. Rev. C*, **55**, 2366 (1997).
- [8] E. Hiyama, B. F. Gibson, and M. Kamimura, *Phys. Rev. C* 70, 031001(R) (2004).
- [9] N. Michel, W. Nazarewicz, and M. Płoszajczak, *Physical Review Letters* 131, 242502 (2023).
- [10] H.M. Hoffmann, and G.M. Hale, *Phys. Rev. C* 77, 044002 (2008).
- [11] K. Arai, S. Aoyama, Y. Suzuki, P. Descouvemont, and D. Baye, *Phys. Rev. Lett.* 107, 132502 (2011).

- [12] S.Aoyama, K. Arai, Y. Suzuki, P. Descouvemont, and D. Baye, Few-Body Syst. 52, 97 (2012).
- [13] A. Cvetinović, D. Đeordić, G. L. Guardo, M. Kelemen, M. La Cognata, L. Lamia, S. Markelj, et al. Physics Letters B, 838 (2023)
- [14] Agata Kowalska, Konrad Czerski, Paweł Horodek, Krzysztof Siemek, Mateusz Kaczmarski, Natalia Targosz-Ślęczka, Mathieu Valat, et al. Materials 16 (2023).
- [15] M. Kaczmarski, et al., Acta Phys. Pol. B 45, 509 (2014).
- [16] K. Czerski, R. Dubey, M. Kaczmarski, A. Kowalska, N. Targosz-Ślęczka, G. Das Haridas, and M. Valat. Physical Review C 109, L021601 (2024).
- [17] H, Gokul Das, R. Dubey, K. Czerski, M. Kaczmarski, A. Kowalska, N. Targosz-Ślęczka, and M. Valat., Measurement 228, 114392(2024).
- [18] S. Agostinelli et al., Geant4 —a simulation toolkit, Nucl. Instrum. Meth. A. 506 , 186 (2003).
- [19] A.H.D. Rasolonjatovo Nuclear Instruments and Methods in Physics Research A 498, 328–333 (2003).
- [20] Y. Nagai, T. Kikuchi, T. Kii, T.S. Suzuki, T. Murakami, T. Shima, T. Ohsaki, Nuclear Instruments and Methods in Physics Research A A 368, 498-502 (1996).
- [21] R. Dubey, et al., Acta Physica Polonica B, 17, 3-A35 (2024).
- [22] <https://www-nds.iaea.org/naa/portal.htmlx>
- [23] Rachid Ouyed, Wojciech R. Fundamenski, Gregory R. Cripps, and Peter G. Sutherland, 501, 367(1998).
- [24] S. Ichimaru, and H. Kitamura, Physics of Plasmas 6, 2649 (1999).

1. Methods

The experiments have been performed at the eLBRUS Ultra High Vacuum Accelerator of the University of Szczecin, Poland. The facility combines a very good vacuum of 10^{-10} mbar in the target chamber with a high current ion beam up to 1 mA on the target [15]. As cross sections of nuclear reactions proceeding far below the Coulomb barrier decrease exponentially with lowering projectile energies, particular attention has been paid to the precise energy definition of the beam provided by the ECR ion source, being of about 10 eV with a long-term stability of about 5 eV. The ion beam is analyzed magnetically and focused by a series of electric lenses to a 7 mm diameter beam spot on the target. In the present experiments, we have applied deuterium D^+ and D^{2+} ion beams with a constant current of 40 μ A and energy ranging between 5 and 20 keV, hitting the deuterium implanted Zr target, known for its stability and high hydrogen stoichiometry ZrD_2 could be achieved.

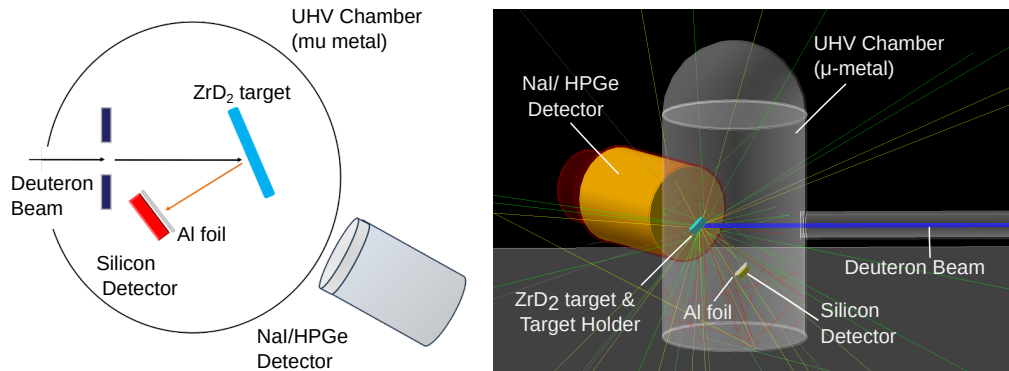


Figure 6: Schematic view of the experimental setup with one silicon detector. Al absorber is placed in front of the Si detector. Large volume NaI(Tl) and HPGe detectors are placed outside the chamber at 115 degrees. Inside view of detection geometry consisting of a silicon detector, target, and target holder simulated with GEANT4 and discussed in detail [17].

To detect high energy electrons/positrons and estimate their branching ratio with protons/neutrons emitted from the DD reaction, we have employed three different kinds of detectors (Fig. 6). For the most precise measurements, we have used single surface-barrier Si detectors of different thicknesses (1, 2, and 3 mm) placed at a distance of 7 cm from the target, at an angle of 135° to the beam. In front of the detectors, Al absorption foils of different thicknesses between 1 and 125 μ m were placed, which enabled the absorption of elastically scattered deuterons as well as heavy charged particles: 0.8 MeV 3He , 1.02 MeV 3H , and 3 MeV protons (see Fig. 1). For comparison, the energy spectrum measured with a very thin Si detector (0.1 mm thick) and an absorption Al foil (1 μ m thick) is presented in Fig. 7. The method of a single Si detector has been already applied in the first measurements and described in detail [16, 17, 21]. The Si detectors were transparent for emitted electrons/positrons of energies up

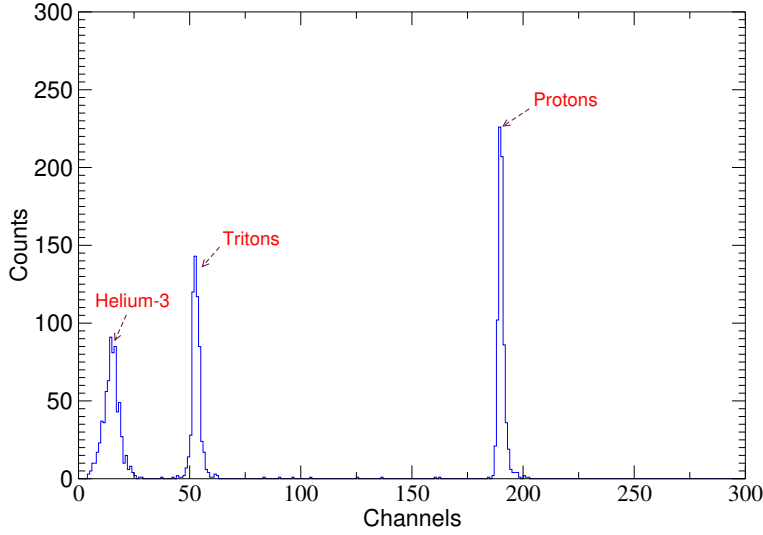


Figure 7: Energy spectrum measured with $100\text{ }\mu\text{m}$ thick Si detector and $1\text{ }\mu\text{m}$ thick Al absorption foil at 10 keV D2 beam. Due to the very small thickness of the detector, no electron/positron bump could be observed.

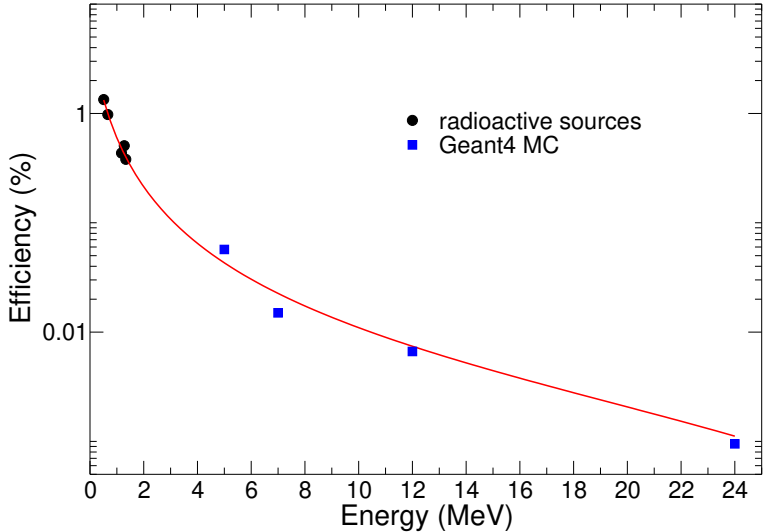


Figure 8: Efficiency curve for a large-volume NaI(Tl) detector (20 cm radius, 25 cm length) with experimental data obtained for different radioactive sources. High energy efficiency was estimated using Geant4 MC simulation, which was verified by existing calibration for the same size detector[25].

to 22.8 MeV so that only the absorption energy line could be observed in the detectors. Since the stopping power of electrons with energies ranging between 1 MeV and 20 MeV is almost constant, the energy absorbed in the detectors varied only slightly and the maximum of the measured energy spectrum was proportional to the detector thickness. Therefore, the continuous e^+e^- energy spectrum could be observed as a distinct absorption bump, strongly improving the effect-to-background ratio. However, to determine the full strength of the IPC transition, Monte Carlo Geant4 simulations were necessary to discern charged particles elastically scattered within the target, target holder, and protective foils [17] (see Fig. 6).

The detection method using a single Si detector cannot present the full energy

spectrum of emitted e^+e^- pairs. Therefore, we have additionally applied a large volume cylindrical NaI(Tl) detector (22 cm diameter, 25 cm length) coupled to 4 separate photomultipliers, which is able to detect the high energy bremsstrahlung related to the 23.84 MeV IPC transition. The NaI(Tl) detector was positioned outside the target chamber at a distance of 32 cm from the target sample. The energy efficiency of the detector was determined using Geant4 MC simulations and fitted to the experimental data obtained for calibration sources: ^{137}Cs , ^{60}Co , and ^{22}Na (see Fig. 8). The efficiency curve has been used to calculate a proper energy spectrum of the bremsstrahlung induced by the internal e^+e^- pair creation and to estimate the excess of positron annihilation events based on the count rate of the 511 keV annihilation line (Fig. 4(a,b)). The final spectral shape of the bremsstrahlung spectrum has been achieved under the assumption of the internal pair creation decay from the 0^+ resonance [16]. The gamma energy spectra obtained during deuteron irradiation of the deuterated Zr target are presented in Fig. 3 and 4 and compared to two different background measurements: with the ion beam on the Faraday cup placed in front of the target chamber and without the ion beam. The high energy region (above 9 MeV) of the latter could be described as the result of cosmic muons similar to ref. [19, 20]. The background in the same energy region measured with the ion beam on the Faraday cup is significantly higher, which arises from the electromagnetic noise induced by the accelerator. In the case of the beam on the target, the noise contribution should be even slightly higher, keeping, however, its energy-independent shape. For the ion beam on the target, the largest contribution at energies higher than 9 MeV results from the bremsstrahlung induced by the IPC transition (see Fig. 3(a)). In the low energy region below 5 MeV, all three spectra are very similar – a considerable increase could only be observed for the annihilation line measured with the beam on the target (Fig. 3(a)). The middle energy region between 5 and 9 MeV is dominated by the known gamma transitions induced by the neutron scattering on sodium and iodine nuclei of the detector [22] and the wall material (μ-metal) of the target chamber (Fig. 3(b)). The neutron response function of all elements of the experimental setup has been simulated with the Geant4 code, adopting the ENDF-VII.0 model as a data set of the cross-section for neutrons [27]. The BROND [28], JEFF [29], and JENDL [30] libraries, which are often used in simulations, show slight discrepancies with our experimental data. The simulated spectra have been smeared with a Gaussian function to reproduce the measured resolution of the NaI crystal, enabling the determination of the number of emitted neutrons from the $^2\text{H}(\text{d},\text{n})^3\text{He}$ reaction at two deuteron energies: 10 and 20 MeV. Measured pulse-height distributions for bremsstrahlung emitted from IPC using the NaI(Tl) detector were unfolded applying Geant4 MC. The validity of the performed Monte Carlo simulations was confirmed with the help of existing works for similar sizes of NaI(Tl) detectors [26].

The low energy gamma spectrum has been also studied with an HPGe detector taking advantage of its much better energy resolution. We have applied a large

volume detector with a 58 mm crystal diameter and 66 mm length providing 35 percent relative efficiency and 2 keV energy resolution (FWHM). The corresponding energy spectrum measured with the deuteron beam on target compared to the background spectra is presented in Fig. 4a and 4b. A large excess of positron annihilation events (511 keV line) could be clearly observed. The absolute efficiency of the HPGe detector could be determined similarly to the method applied for the NaI(Tl) detector based on the radioactive calibration sources and Geant4 MC simulations. The simulation calculations have shown that the contribution to the annihilation line arising from external pair creation is at least two orders of magnitude weaker than observed. Since the neutron-induced gamma spectrum in the middle energy region between 5 and 9 MeV was much weaker than that measured with the scintillator detector, we could only determine the branching ratio between IPC and the proton channel determined simultaneously using the Si detector.

References

- [25] Bruce A. Faddegon, et al, Nuclear Instruments and Methods in Physics Research A 301, 138-149 (1991).
- [26] C. W. Sandifer and M. Taherzadeh, IEEE Transactions on Nuclear Science, 15, 336-345 (1968).
- [27] M.B. Chadwick, et al., ENDF/B-VII. 0: next generation evaluated nuclear data library for nuclear science and technology, Nucl. Data Sheets 107, 2931–3060 (2006).
- [28] A.I. Blokhin, E.V. Gai, A.V. Ignatyuk, I.I. Koba, V.N. Manokhin, V.G. Pronyaev, New version of neutron evaluated data library BROND-3.1, Probl. Atom. Sci. Technol. Ser.: Nucl. React. Constants 2, 2–5 (2016).
- [29] A A.J.M. Plompen, O. Cabellos, C. De Saint Jean, M. Fleming, A. Algora, M. Angelone, P. Archier, E. Bauge, O. Bersillon, A. Blokhin, F. Cantargi, The joint evaluated fission and fusion nuclear data library, JEFF-3.3, Eur. Phys. J. A 56 (7), 181 (2020).
- [30] O. Iwamoto, K. Shibata, N. Iwamoto, S. Kunieda, F. Minato, A. Ichihara, S. Nakayama, Status of the JENDL project, in: In EPJ Web of Conferences, vol. 146, 02005 (2017).
- .